

# High Frame Rate Imaging to Enhance the Dissolution of Histotripsy-Induced Bubble Clouds

Kenneth B. Bader  
Department of Radiology,  
Committee on Medical Physics  
University of Chicago  
Chicago, IL USA  
baderk@uchicago.edu

Paul G. Severino  
Department of Physics  
University of Chicago  
Chicago, IL USA  
paulseverino@uchicago.edu

Samuel A. Hendley  
Committee on Medical Physics  
University of Chicago  
Chicago, IL USA  
hendley@uchicago.edu

Gregory A. Anthony  
Committee on Medical Physics  
University of Chicago  
Chicago, IL USA  
ganthony@uchicago.edu

Viktor Bollen  
Department of Radiology  
University of Chicago  
Chicago, IL USA  
bollen@uchicago.edu

**Abstract**— Histotripsy is a focused ultrasound therapy for tissue ablation with bubble cloud activity. Persistent bubble clouds reduce the ablative capacity of histotripsy. Thus, there is a need for bubble-specific imaging to track bubble cloud dissolution between the application of histotripsy pulses. In this study, standard plane wave, pulse inversion, and chirp-coded excitation imaging were utilized to visualize bubble clouds at a 2-kHz frame rate. For all imaging schemes, a monotonic decrease in the bubble cloud grayscale was observed over a 45-ms period following the histotripsy insonation. The change in bubble cloud grayscale was dependent on the imaging scheme, with faster grayscale reduction for larger peak negative pressures of the imaging pulse. Bubble-specific sequences resulted in faster decreases in the bubble cloud grayscale compared with standard plane wave imaging. Overall, these results highlight high-frame rate imaging as a means to monitor and modulate histotripsy bubble cloud dissolution.

**Keywords**—histotripsy, plane wave imaging, contrast imaging

## I. INTRODUCTION

Ultrasound as a therapeutic modality has been under development since the 1950s [1]. Histotripsy is a focused ultrasound therapy that imparts lethal mechanical damage to the target tissue via the generation of bubble clouds [2], and has the potential to translate for the ablation of numerous pathologies [3]. Bubble clouds that persist between histotripsy pulses generate damage at discrete locations within the focal zone, leading to an incomplete tissue disintegration [4]. Thus, there is a need to ensure the dissolution of bubble clouds between the application of consecutive histotripsy pulses.

Diagnostic ultrasound imaging is the primary modality for monitoring the hyperechoic histotripsy bubble cloud. Conventional B-mode requires tens of milliseconds for image acquisition, over which time the bubble cloud can undergo significant changes and multiple histotripsy pulses may be applied [5]. Standard plane wave imaging employs all elements in parallel to transmit and receive echoes, shortening the acquisition sequence to less than 100  $\mu$ s.

This work was funded in part by the National Institutes of Health, Grant R01 HL133334 and the University of Chicago Comprehensive Cancer

The standard plane wave sequence temporal resolution is sufficient to track bubble cloud dissolution [6], providing a potential means to provide feedback for the histotripsy application rate. The imaging pulse interacts with the bubble cloud, resulting in a faster reduction in bubble cloud grayscale with larger peak negative pressures [6]. Standard plane wave imaging lacks bubble-specific contrast. Such contrast would facilitate bubble cloud detection in an *in vivo* heterogeneous environment. The nonlinear oscillations induced by bubble-specific imaging sequences may also accentuate cloud dissolution [7].

In this study, histotripsy bubble clouds generated in a tissue mimicking phantom were monitored with high frame rate imaging. Sequences that were bubble inspecific (standard plane wave) and bubble specific (pulse inversion and chirp-coded excitation) were explored. For each sequence, the contrast-to-noise ratio and time-dependent bubble cloud grayscale were tracked.

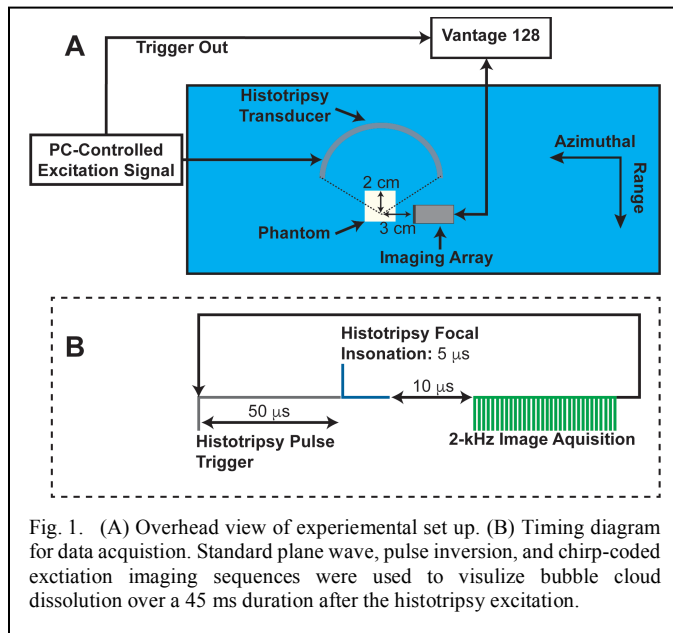
## II. METHODS AND MATERIALS

### A. Experimental Set-up

A focused source (1-MHz fundamental frequency, 7.5-cm focal distance, 10-cm diameter) driven by a class D amplifier [8], [9] was used to generate bubble clouds in a tissue mimicking phantom [10]. Pulses of 5- $\mu$ s duration and 25-MPa peak negative pressure were applied at a 10-Hz rate. An L11-5v imaging array controlled by a research ultrasound system (Vantage 128, Verasonics, Kirkland, WA, USA) was oriented to monitor bubble cloud activity along the central axis of the therapy source (**Fig. 1**). The sequence acquired images at a 2-kHz frame rate over a 45-ms duration following the histotripsy excitation (**Fig. 1B**).

### B. Imaging Sequences

The bubble clouds were monitored with either standard plane wave, pulse inversion, or chirp-coded excitation schemes. For the plane wave and pulse inversion acquisitions, the imaging



pulse had a 5-MHz fundamental frequency and 0.3- $\mu$ s pulse duration. For chirp-coded excitation imaging, the pulse bandwidth ranged from 4.8 to 6 MHz over a 2- $\mu$ s duration. For all sequences, the electrical excitation to the imaging array was either 5 or 25 V. Images were downloaded and processed offline. The threshold grayscale value separating the bubble cloud from background was determined via Otsu's method. For each frame (i.e. timepoint), the bubble cloud area and mean grayscale value was tabulated.

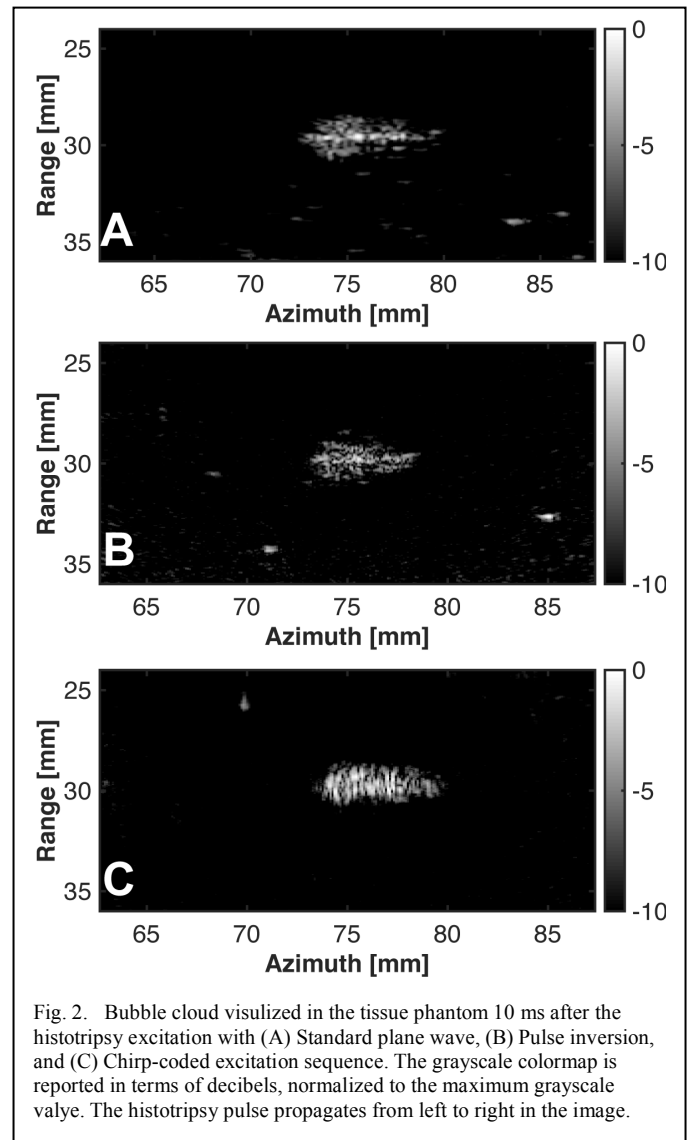
### III. RESULTS

#### A. Bubble cloud tracking

Bubble clouds generated within the phantom were readily visualized for all tested modalities, as indicated in **Fig. 2**. For a given voltage applied to the imaging array, no difference was observed in the bubble cloud area between the three imaging schemes ( $p > 0.05$  by ANOVA analysis with Tukey HSD *post hoc* correction). The contrast-to-noise ratio was also not significantly different between the imaging schemes. Both the bubble cloud area and contrast-to-noise ratio were evaluated 10 ms following the histotripsy insonation.

#### B. Bubble cloud dissolution profile.

The 2-kHz frame rate utilized in this study had sufficient temporal resolution to track bubble cloud dissolution accurately (**Fig. 3**). A slow change in the mean bubble cloud grayscale was observed over the 45 ms observation window with all imaging schemes, with an overall reduction in the bubble cloud grayscale by 50–80%. To characterize the dissolution rate, the time to a 50% reduction in the bubble cloud grayscale was tabulated for all experimental conditions (**Fig. 4**). A larger electrical signal applied to the imaging array resulted in a significant reduction in the time to 50% bubble cloud grayscale for all the tested imaging sequences ( $p < 0.05$ ). For a given voltage to the imaging array, the time to 50% bubble cloud grayscale was on average shorter for the bubble-specific imaging sequences compared to the standard plane wave imaging sequence. Chirp-coded



excitation imaging had the shortest observed time to a 50% reduction in bubble cloud grayscale.

### IV. DISCUSSION AND CONCLUSIONS

In this study, histotripsy-generated bubble clouds were visualized following the therapeutic excitation with standard plane wave, pulse inversion, and chirp-coded excitation imaging sequences. Because of the relatively long dissolution time [6], the 2-kHz frame rate employed in this study was sufficient to provide accurate tracking of the bubble cloud over the 45 ms observation window. Implementing high-speed feedback based on the bubble cloud grayscale during the application of histotripsy pulses would minimize the so-called cavitation memory effect to ensure uniform ablation of the target tissue [4]. Such an imaging sequence could complement coalescing bubble sequences [11], or be employed on its own to reduce the burden of residual bubble clouds [6].

The pulse inversion and chirp-coded excitation sequences form images based on bubble-specific second harmonic emissions, and should provide strong contrast of the bubble

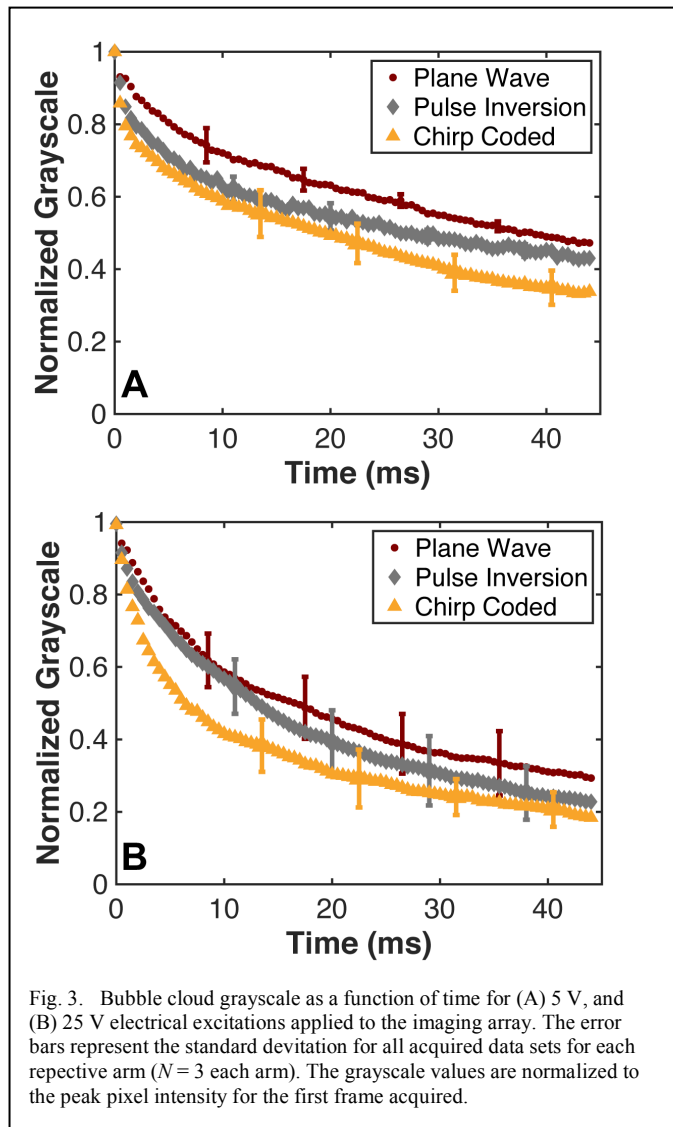


Fig. 3. Bubble cloud grayscale as a function of time for (A) 5 V, and (B) 25 V electrical excitations applied to the imaging array. The error bars represent the standard deviation for all acquired data sets for each respective arm ( $N = 3$  each arm). The grayscale values are normalized to the peak pixel intensity for the first frame acquired.

cloud compared to standard plane imaging. No differences were noted in the contrast-to-noise ratio for the imaging schemes investigated here. This may be in part due to the low scatter phantom employed in this study [10], which resulted in a uniformly hypoechoic background. Future studies will investigate the ability of each of these schemes to identify bubble clouds in a heterogeneous environment *in vivo*. The nature of histotripsy bubble activity may also have been a contributing factor in the observed similarity of the contrast-to-noise ratio between the imaging schemes. Histotripsy pulses can generate bubbles greater than 100  $\mu\text{m}$  in diameter [12]. Bubbles of this size may scatter the imaging pulse geometrically [13], resulting in a relatively small nonlinear signal.

The bubble cloud dissolution profile was influenced by the imaging parameters, as indicated by the variation in the time to a 50% reduction in bubble cloud grayscale (Fig. 4). The peak negative pressure of the imaging pulse, proportional to the voltage applied to the imaging array, influenced the rate of reduction in bubble cloud grayscale, consistent with a previous observation [6]. The type of imaging scheme also influenced the bubble cloud behavior, with chirp-coded excitation schemes

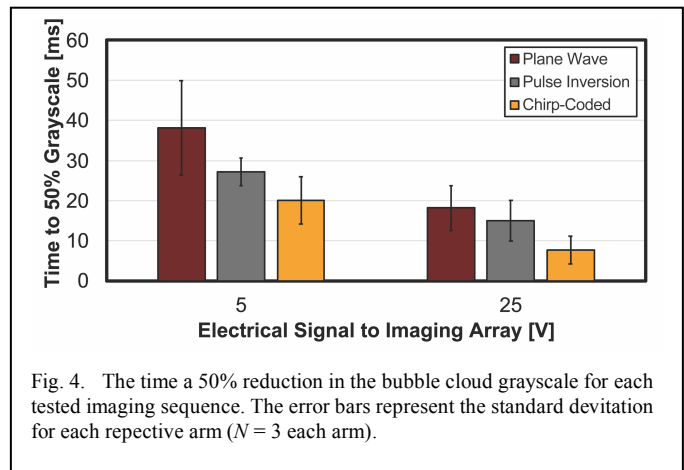


Fig. 4. The time a 50% reduction in the bubble cloud grayscale for each tested imaging sequence. The error bars represent the standard deviation for each respective arm ( $N = 3$  each arm).

resulting in the shortest time to a 50% reduction in the bubble cloud grayscale, and standard plane wave imaging resulting in the longest time. There may be multiple reasons for this observation. The nonlinear bubble oscillations accentuated by bubble-specific sequences and increased peak negative pressure of the imaging pulse will enhance the diffusion of gas into the surrounding medium [7]. The duration of the pulse inversion and chirp-coded excitation schemes are two and ten times longer, respectively, than the standard plane wave sequence. The extended duration of the bubble-specific sequences may generate sustained nonlinear bubble oscillations and therefore a faster cloud dissolution rate [13]. The population of bubbles producing contrast from the bubble-specific sequences will also vary from the standard plane wave sequences, which may also account for the discrepancy in the observed bubble cloud dissolution profile.

Overall, these results indicate the utility of bubble-specific imaging sequences for monitoring histotripsy bubble cloud dissolution. When implemented as a high frame rate sequence, these imaging methods will provide the necessary feedback for the application of histotripsy pulses for uniform disintegration of the target tissue.

#### REFERENCES

- [1] W. D. O'Brien Jr and F. Dunn, "An early history of high-intensity focused ultrasound," *Phys. Today*, vol. 68, no. 10, pp. 40–45, Oct. 2015.
- [2] K. B. Bader, E. Vlaisavljevich, and A. D. Maxwell, "For Whom the Bubble Grows: Physical Principles of Bubble Nucleation and Dynamics in Histotripsy Ultrasound Therapy," *Ultrasound Med. Biol.*, vol. 45, no. 5, pp. 1056–1080, May 2019.
- [3] V. A. Khokhlova, J. B. Fowlkes, W. W. Roberts, G. R. Schade, Z. Xu, T. D. Khokhlova, T. L. Hall, A. D. Maxwell, Y.-N. Wang, and C. A. Cain, "Histotripsy methods in mechanical disintegration of tissue: Towards clinical applications," *Int. J. Hyperthermia*, vol. 31, no. 2, pp. 145–162, Mar. 2015.

- [4] T.-Y. Wang, Z. Xu, T. L. Hall, J. B. Fowlkes, and C. A. Cain, "An Efficient Treatment Strategy for Histotripsy by Removing Cavitation Memory," *Ultrasound Med. Biol.*, vol. 38, no. 5, pp. 753–766, May 2012.
- [5] A. D. Maxwell, T.-Y. Wang, C. A. Cain, J. B. Fowlkes, O. A. Sapozhnikov, M. R. Bailey, and Z. Xu, "Cavitation clouds created by shock scattering from bubbles during histotripsy," *J. Acoust. Soc. Am.*, vol. 130, no. 4, p. 1888, 2011.
- [6] K. B. Bader, S. A. Hendley, G. J. Anthony, and V. Bollen, "Observation and modulation of the dissolution of histotripsy-induced bubble clouds with high-frame rate plane wave imaging," *Phys. Med. Biol.*, vol. 64, no. 11, pp. 115012–15, Jun. 2019.
- [7] C. C. Church, "Prediction of rectified diffusion during nonlinear bubble pulsations at biomedical frequencies," *J. Acoust. Soc. Am.*, vol. 83, no. 6, pp. 2210–2217, Jan. 1988.
- [8] T. Hall and C. Cain, "A low cost compact 512 channel therapeutic ultrasound system for transcutaneous ultrasound surgery," *AIP Conf. Proceed.*, vol. 829, p. 445, 2006.
- [9] A. D. Maxwell, P. V. Yuldashev, W. Kreider, T. D. Khokhlova, G. R. Schade, T. L. Hall, O. A. Sapozhnikov, M. R. Bailey, and V. A. Khokhlova, "A Prototype Therapy System for Transcutaneous Application of Boiling Histotripsy," *IEEE Trans. Ultrason., Ferroelect., Freq. Contr.*, vol. 64, no. 10, pp. 1547–1557, Aug. 2017.
- [10] K. B. Bader, M. J. Crowe, J. L. Raymond, and C. K. Holland, "Effect of Frequency-Dependent Attenuation on Predicted Histotripsy Waveforms in Tissue-Mimicking Phantoms," *Ultrasound Med. Biol.*, vol. 42, no. 7, pp. 1701–1705, Jul. 2016.
- [11] A. Shi, J. Lundt, Z. Deng, J. Macoskey, H. Gurm, G. Owens, X. Zhang, T. L. Hall, and Z. Xu, "Integrated Histotripsy and Bubble Coalescence Transducer for Thrombolysis," *Ultrasound Med. Biol.*, vol. 44, no. 12, pp. 2697–2709, Sep. 2018.
- [12] E. Vlaisavljevich, K.-W. Lin, M. T. Warnez, R. Singh, L. Mancina, A. J. Putnam, E. Johnsen, C. Cain, and Z. Xu, "Effects of tissue stiffness, ultrasound frequency, and pressure on histotripsy-induced cavitation bubble behavior," *Phys. Med. Biol.*, pp. 2271–2292, Feb. 2015.
- [13] K. B. Bader and C. K. Holland, "Gauging the likelihood of stable cavitation from ultrasound contrast agents," *Phys. Med. Biol.*, vol. 58, no. 1, pp. 127–144, Dec. 2012.